Surgically assisted rapid palatal expansion: is the pterygomaxillary disjunction necessary? A finite element study

Osman Koç, and Helder Baldi Jacob

Transverse discrepancy is an important factor in determining facial esthetics. It has been shown there is an inverse correlation between the buccal corridor width and the intercanine and intermolar widths. Despite the fact midpalatal expansion is the treatment of choice for growing subjects, for skeletally mature subjects the rapid palatal expansion has limited orthopedic effects, and surgically assisted rapid palatal expansion (SARPE) is preferred. SARPE has shown inconsistencies depending on the surgical technique and/or expander device design. Some authors suggest that median and lateral osteotomies are sufficient to achieve the desired transverse dimensions using the SARPE procedure, while others recommend additional surgical separation of the pterygomaxillary junction. There are still controversies regarding the pterygomaxillary sutures (PMS) disjunction effect. Therefore, this study aimed to evaluate the displacement and stress distribution of the craniofacial structures resulting from SARPE, either with or without PMS osteotomy, using two different expander design (tooth-borne and tooth-bone-borne) using finite element method and finite element analysis (FEM/FEA). Regardless of the maxillary expander device type, both SARPE surgical techniques effectively produced maxillary expansion. SARPE with PMS osteotomy presented parallel maxillary expansion, and reduced stress values in the craniofacial and maxillofacial structures. (Semin Orthod 2022; 28:227–242) ***© 2022 Elsevier Inc. All rights reserved.***

Introduction

Attractiveness is important for individuals to increase their self-confidence, social acceptance, popularity, and career successes.[1,2] Facial esthetics is a part of dentistry, and orthodontists play an important role in determining the patient's facial esthetics. Improving facial and smile esthetic has become an important goal in orthodontic treatment.

The transverse width of the smile is also an important factor in determining facial esthetics. The literature has reported that minimal or excessive buccal corridors (black spaces between the posterior teeth and inner part of the cheeks) can be considered less attractive.[3–5] Although inconsistencies have been shown in regards the influence of the buccal corridors to the smile esthetics,[5–9] it has been reported there is an inverse correlation between the buccal corridor with intercanine and intermolar widths.[10,11]

Transverse deficiency, such as a narrow maxilla, with or without posterior crossbite, is a common dental problem. It has been reported that maxillary transverse deficiency increases from the American children to the American adult population (7.0% to 9.5%, respectively).[12] The treatment of maxillary transverse discrepancy (MTD) varies depending on the degree of the

Department of Mechanical Engineering, Yildiz Technical University, Barbaros Boulevard, Yildiz, Istanbul 34349, Turkey; Department of Orthodontics, The University of Texas Health Science Center at Houston School of Dentistry, 7500 Cambridge St. Suite 5130, Houston, TX 77054, USA.

Correspondent author. E-mail: helder.b.jacob@uth.tmc.edu

© 2022 Elsevier Inc. All rights reserved.

1073-8746/12/1801-$30.00/0

https://doi.org/10.1053/j.sodo.2022.10.017

transverse and anteroposterior deficiencies of the maxilla, and the patient's age.[13] Despite the fact midpalatal expansion is the treatment of choice for growing subjects, for skeletally mature subjects the rapid palatal expansion (RPE) has limited orthopedic effects, and surgically assisted rapid palatal expansion (SARPE) is prefered.[14]

The goal of transverse expansion is to maximize the skeletal effect while minimizing the dental ones. Various maxillary expander devices have been used for the palatal expansion. It is important for the clinician to choose the best design and position of the maxillary expander device for the most desirable outcome.[15,16] Recently, the use of miniscrew assisted rapid palatal expansion (MARPE) has increased the maxillary expander design armamentarium, and successful midpalatal distraction with these expanders has been described with minimum side effects to teeth and periodontium.[17,18]

Although non-surgical palatal expansion is possible in adult and young adult patients, the stability is low.[19,20] When orthopedic maxillary expansion fails due to high sutural resistance or the MTD is greater than 5 mm, SARPE is the preferred procedure.[21,22] The aim of surgical osteotomy is to facilitate transverse enlargement and to prevent the formation of mini-fractures and cracks that may occur due to stresses in the craniofacial and maxillofacial structures.[23] It has been reported that the midpalatal, zygomaxillary, and pterygomaxillary sutures are areas of resistance during maxillary expansion.[24] Therefore, a surgical approach reduces the sutural resistance releasing the palatal plates from the circumpalatal sutures and offers a true orthopedic maxillary expansion.[14,25–28] Some surgical techniques have been proposed to mobilize the maxillary halves.[29–35]

Some authors have suggested that median and lateral osteotomies are sufficient to achieve the desired transverse dimensions using the SARPE procedure.[30,32,36–38] However, others have argued that in addition to these osteotomies, pterygomaxillary sutures (PMS) disjunction should be performed.[27,39–41] There are still controversies regarding the PMS disjunction effect. Therefore, the aim of this study was to evaluate the displacement and stress distribution of the craniofacial structures resulting from SARPE, either with or without PMS disjunction, using two different expander design (tooth-borne and tooth-bone-borne) using finite element method (FEM) and finite element analysis (FEA).

Material and methods

A finite element model was generated using an anatomical model of a young adult (22-year-old male was 172.8 cm height and weighted 65.0 kg) obtained from an anatomagraphic database developed from magnetic resonance imaging (MRI).[42,43] Each image of the head featured a slice thickness of 2 mm (256×256×240 mm), and additional anatomical segmentations were introduced in the original data.[44,45]

Using ANSYS software, all of the skull's bones (craniofacial and maxillofacial bones), and teeth were downloaded in STL format (19.3, ANSYS Inc. Houston, PA, USA). All bones were combined except for the maxilla in a Boolean operation using Ansys software. A symmetrical model of the craniofacial and maxillofacial structures with the maxilla, teeth, and periodontal ligaments included independently in the overall model was created for FEA (Fig. 1).

The final model (Fig. 2) was edited and generated using Mimics software (version 15.0; Materialise, Leuven, Belgium). The offset command was used to model the periodontal ligament (PDL) with a thickness of 0.20 mm.[46] Anisotropic materials were periodontal ligament, cortical, and cancellous bone. Homogeneous and isotropic materials were considered tooth and stainless steel. The hyperelastic material (third order Ogden) model was used to describe PDL (Table 1).[47–49]

In FEA, four scenario models were designed using two different surgical osteotomy techniques (median and lateral osteotomies, with and without PMS disjunction) and two different expansion appliances to compare the simulation results. A tooth-born expansion appliance (Hyrax) attached to the maxillary first molar associated with palatal canine double arm extension was modeled (Fig. 3A); a tooth-bone-borne palatal expander type (miniscrew assisted rapid palatal expansion - MARPE), containing four miniscrews implants (MSIs) placed at 4.00 mm lateral from the midpalatal suture, was attached to maxillary first molars was modeled (Fig. 3B). MSIs (1.60 mm diameter and 10.00 mm length) were modeled with ANSYS Software. The expander was activated transversely 2.5 mm in the palatal expansion simulation (a total of 5.00 mm). Model-I and Model-II simulated

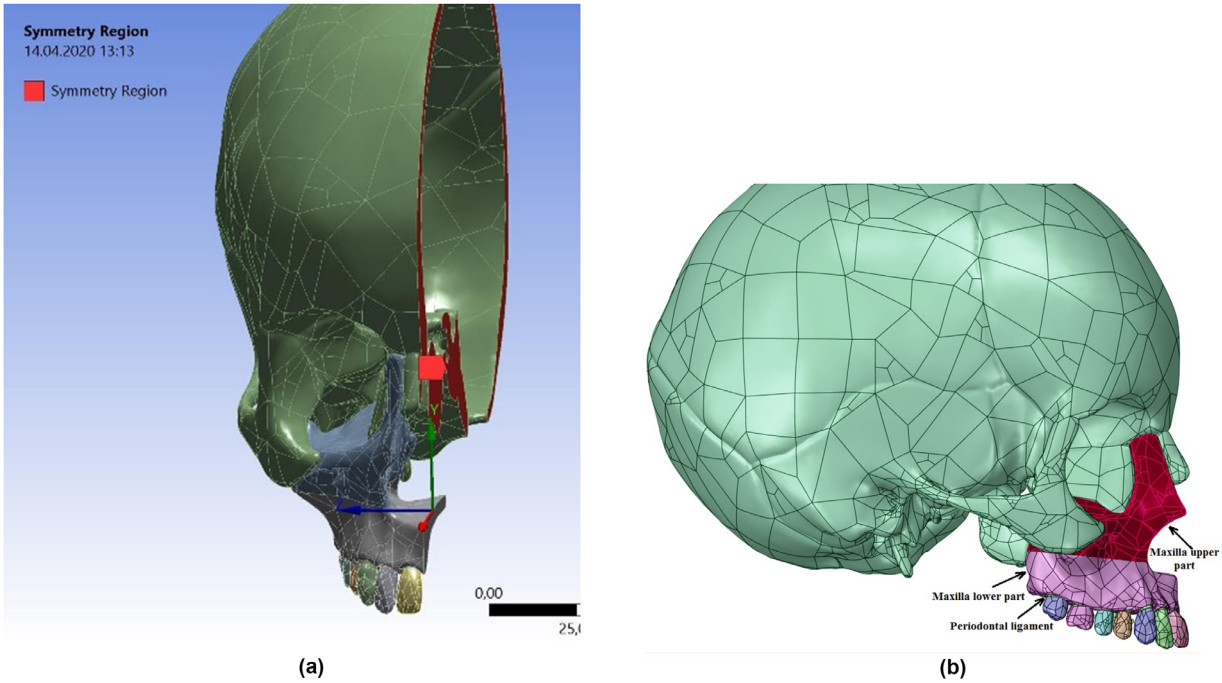


Fig. 1. Symmetrical model of the craniofacial and maxillofacial structures (A) with the maxilla, teeth, and periodontal ligaments created independently (B).

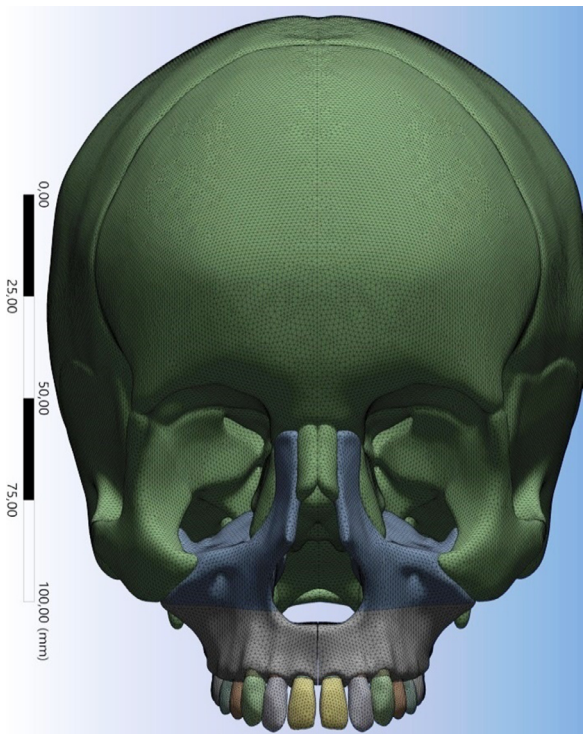


Fig. 2. Overall finite element model.

Table 1. Finite element model's material properties.

Material properties (Mpa)			
Cortical Maxillary bone	Ex:12000	Vxy: 0.18	Gxy: 3600
	Ey: 11640	Vyz: 0.40	Gyz: 5400
	Ez: 15600	Vxz: 0.30	Gxz: 4100
Cortical Skull bone	Ex: 12580	Vxy: 0.48	Gxy: 4400
	Ey: 13600	Vyz: 0.24	Gyz: 6700
	Ez: 21200	Vxz: 0.32	Gxz: 4900
Cancellous bone	Ex:1148	Vxy: 0.32	Gxy: 434
	Ey: 1148	Vyz: 0.05	Gyz: 68
	Ez: 210	Vxz: 0.05	Gxz: 68
Periodontal Ligament	$\mu_{1:}$ - 3420.83	$\mu_{2:}$ 1434.35	$\mu_{3:}$ - 5.56E-04
	$\alpha_{1:}$ - 0.506	$\alpha_{2:}$ - 0.134	$\alpha_{3:}$ 13.708
	$D_{1:}$ 0 MPa^{-1}	$D_{2:}$ 0 MPa^{-1}	$D_{3:}$ 0 MPa^{-1}
Dentin	19890	0.31	
Stainless steel	193000	0.35	

MPa: Megapascal
Ex, Ey, Ez: Elastic modulus in three directions.
Vxz, Vyz, Vxz: Poisson's ratio in three directions.
Gxy, Gyz, Gxz: Shear modulus in three directions.
μ, α, D : Material parameters

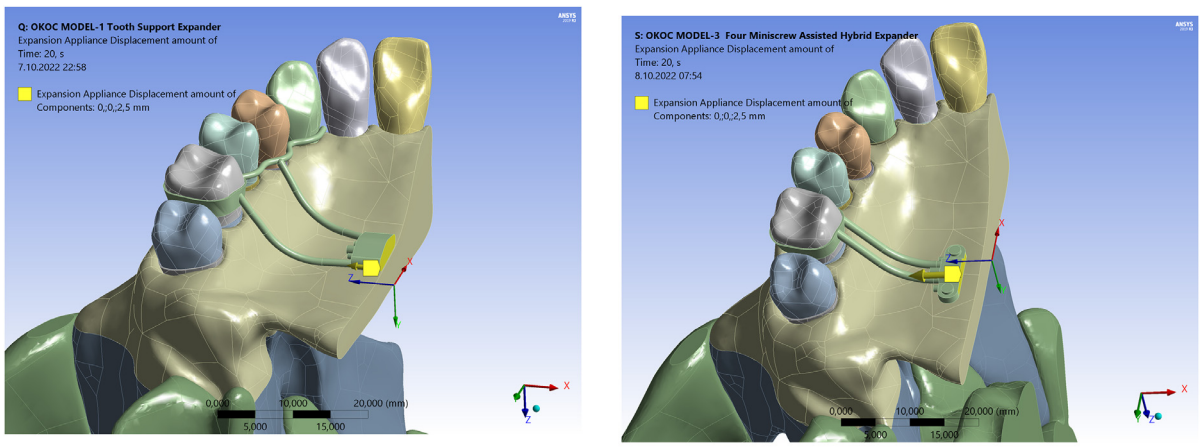
the changes of maxillary expansion with the Hyrax (median and lateral osteotomies, without and with PMS disjunction, respectively); Model-III and Model-IV simulated the maxillary expansion with the MARPE (median and lateral osteotomies, without and with PMS disjunction, respectively).

Various skeletal and dental signs were incorporated in this study. The dental landmarks were as follows: central and lateral incisors, canine, first and second premolars, and first and second molars. Skeletal landmarks were as follows: anterior nasal spine (ANS), posterior nasal spine (PNS), frontomaxillary suture, zygomaticomaxillary suture, frontozygomatic suture, zygomatic arc, medial pterygoid plate, lateral pterygoid plate. The foramen magnum was considered a completely fixed and stable point.[50] Rotation and typing of the maxilla were measured in all three planes.

Boundary conditions

The transverse displacement of the craniofacial and maxillofacial structures was evaluated along the X, Y, and Z coordinates. The X-axis evaluated coronal plane changes, the Y-axis evaluated axial plane changes, and the Z-axis evaluated sagittal plane changes. Stress areas were assessed using a distinct color scale band gap. Positive and negative values in the stress spectrum column represent tension and compression, respectively. The stress distribution was calculated in Mega-Pascal (MPa) using the von Mises criterion, and the displacement was measured in millimeters (mm). A time-dependent dynamic analysis (transient structural analysis) type and nonlinear analysis (three theories) method (geometric, contact, and material methods) were used. In all models, displacement and stress values on the same element were measured with ANSYS software using a measuring probe.

The displacement movement was transmitted to the maxilla via the expansion appliance screw, which was activated 0.25 mm per step. Transverse displacement of 2.50 mm in the Z-axis corresponding to 5.00 mm of travel was achieved in the symmetrical FEA model. The results were obtained after a total activation of the expansion



(a) (b)

Fig. 3. Two different palatal expander appliances design: tooth-borne expander (A), and tooth-bone-borne (B). Screw were moved 2.5 mm in a transverse (Z-axis) direction (5 mm in total).

screw of 5 mm. Between the maxillary surfaces separated by lateral osteotomy, frictionless contact was defined. Bonded contacts were defined between the teeth, the periodontal ligament and the screw of the expansion appliance and the maxilla. Frictional contact was defined between the contacting surfaces in models with PMS disjunction (friction coefficient 0.3). The surfaces in contact with the sphenoid bone of the lower part of the maxilla, separated by lateral osteotomy, were selected. They move as a single unit, with no separation or sliding of the faces and edges were permitted. The angular changes made by the line passing through the nodes between the ANS and PNS points with respect to the symmetrical plane of the skull were used to measure the amount of rotation of the maxilla.

Mesh structure affects the accuracy of the study in FEM/FEA. For this, it is desirable to check the correct size and the number of models are divided into elements. In the study, mesh convergence was performed to accurately measure the stress value, and the mesh refinement process was performed on the sphenoid bone and maxilla surface, which were in contact, by choosing 1.3 mm and 1 mm mesh element sizes, respectively. It has been observed that the elemental mean stress values of the elements in the region where the stress is maximum in the mesh convergence range (although the mesh size is reduced) do not change more than 6%. The optimum number of elements was determined for the best mesh convergence in the model.

Finite element model

Quadratic tetrahedral and hexahedral elements were used for volumetric mesh generation, and the FEA model was composed of 2,196,327 nodes and 1,398,813 elements. The maxilla, PDL, and tooth contained more fine elements than elsewhere of the skull (Fig. 2). The expansion device and the anchor screw, PDL and tooth are divided into hexahedral elements (Table 2). Element and node count and mesh size values were the same for all models, and the mean mesh skewness element quality convergence value was set to 0.28 (Table 2).

Results

Displacement amount

Regardless of the appliance, median and lateral osteotomies with PMS disjunction presented more parallel transverse displacement (Table 3). Model-I (Fig. 4) presented a transverse V-shaped displacement difference between of ANS (2.961 mm) and PNS (0.431 mm) of 2.530 mm. Model-II (Fig. 5) showed a parallel transverse displacement with the ANS and PNS shift of 2.500 mm and 2.490 mm, respectively. The transverse V-shaped displacement was also observed for the Model-III (Fig. 6) with difference between ANS (3.218 mm) and PNS (1.722 mm) being of 1.496 mm. The Model-IV (Fig. 7) showed the same transverse displacement of ANS and PNS (2.500 mm, for both). The craniofacial structures present a small similar displacement (Table 3 and Figs. 4–7).

Model-I (Fig. 4) and Model-III (Fig. 6) showed a dental transverse displacement decreasing gradually from the central incisor to the second molar. On the other hand, the transverse dental displacement measured on Model-II (Fig. 5) and Model-IV (Fig. 7) were similar from central incisors to second molars, due to practically parallel opening of the midpalatal suture. All Models presented their largest dental displacement at the central incisors and the smallest at the second molars (Table 3); Model-III (Fig. 6) followed by Model-I (Fig. 4) showed the largest values for central incisors (4.280 mm and 3.700 mm, respectively). Model-I (Fig. 4) presented

Table 2. Finite element model's element, nodes, mesh size and average skewness element quality convergence values.

	Average skewness value	*Nodes*	*Element*	*Mesh size (milimeters)*	*Mesh Element Type*
Skull	0.19	1691902	1158657	1.80	Tetrahedral
Maxilla (inferior part)	0.17	105921	71404	1.30	Tetrahedral
Maxilla (superior part)	0.15	104642	71184	1.30	Tetrahedral
Periodontal ligament	0.50	116542	41668	0.40	Hexahedral
Tooth	0.45	155741	49998	0.60	Hexahedral
Tooth supported (hyrax) palatal expander	0,50	21579	5470	0.40	Hexahedral
Tooth-bone-borne palatal expander	0.50	20017	5233	0.40	Hexahedral

Table 3. Unilateral displacements (mm) of the evaluated landmarks after 5 mm of the maxillary expander activation.

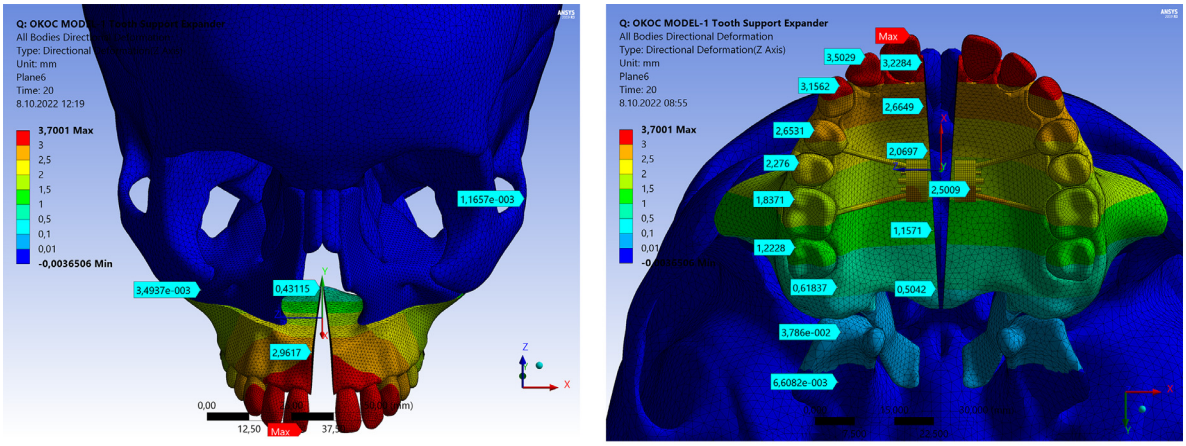
	Model-I			*Model-II*			*Model-III*			*Model-IV*		
Anatomical structure	*X-Axis*	*Y-Axis*	*Z-Axis*	*X-Axis*	*Y-Axis*	*Z-Axis*	*X-Axis*	*Y-Axis*	*Z-Axis*	*X-Axis*	*Y-Axis*	*Z-Axis*
Central incisor	0.370	-1.109	3.700	0.005	0.002	2,507	-0.243	-0.289	4.280	0.000	0.000	2.500
Lateral incisor	-0.093	-0.895	3.502	0.003	0.002	2.506	-0.521	0.045	4.186	0.000	0.000	2.500
Canine	-0.429	-0.694	3.156	0.001	0.002	2.505	-0.712	0.317	3.949	-0.000	-0.000	2.500
First premolar	-0.604	-0.534	2.653	0.000	0.001	2.502	-0.817	0.520	3.648	-0.000	-0.000	2.500
Second premolar	-0.776	-0.373	2.276	-0.001	0.000	2.501	-0.929	0.684	3.410	-0.000	-0.000	2.500
First molar	-0.831	-0.273	1.837	-0.001	-0.001	2.499	-0.965	0.806	3.146	-0.000	-0.000	2.500
Second molar	-0.784	-0.104	1.222	-0.002	-0.003	2.495	-0.781	0.710	2.645	-0.000	-0.000	2.500
Anterior nasal spine	0.994	-1.079	2.961	0.000	0.000	2.500	0.156	-0.381	3.217	0.000	0.000	2.500
Posterior nasal spine	1.074	-0.457	0.431	0.000	-0.009	2.490	0.193	-0.065	1.722	0.000	-0.000	2.500
Frontomaxillary suture	0.011	-0,031	0.000	-0.000	0.000	-0.000	-0.483	1.009	-0.001	-0.000	0.000	0.000
Zygomaticomaxillary suture	0.002	-0.022	0.003	0.000	0.000	0.000	0.104	1.159	0.209	-0.000	0.000	0.000
Frontozygomatic suture	0.012	-0.023	0.001	-0.000	0.000	-0.000	-0.620	1.003	0.017	-0.000	0.000	0.000
Zygomatic arch	0.004	-0.014	0.001	0.000	0.000	-0.000	-0.226	0.662	-0.007	-0.000	0.000	0.000
Medial pterygoid plate	-0.045	-0.013	0.037	-0.000	0.000	0.000	-0.346	0.856	0.913	-0.000	0.000	0.000
Lateral pterygoid plate	-0.013	-0.013	0.006	0.000	0.000	0.000	-0.247	0.654	0.266	-0.000	0.000	0.000
Foramen magnum	0.000	0.000	0.000	0.000	0.000	0.000	0.000	0.000	0.000	0.000	0.000	0.000
Angle of rotation and tipping	0.86°	1.04°	-3.39°	-1e-2°	8e-3°	-1e-2°	0.38°	1.82°	-1.98°	1e-5°	-1e-3°	-5e-5°

Obs.: X-axis, coronal plane; Y-axis, axial plane; Z-axis, sagittal plane. Positive (+) values indicate forward, outward or upward displacement, and negative (−) values indicate backward, inward or downward displacement. Median and lateral osteotomies were made in all models without pterygomaxillary suture separation.

the smallest transverse second molar displacement (1.222 mm), while Model-II (Fig. 5), Model-III (Fig. 6), and Model-IV (Fig. 7) displayed similar amount for the second molar (approximately 2.500 mm).

Stress distribution

Model-III (Fig. 10) showed the highest stress distribution value for all craniofacial structures, and Model-I (Fig. 8) showed the lowest stress distribution value in general (Table 4). Model-II (Fig. 9) and Model-IV (Fig. 11) presented stress values nearly zero (Table 4). Model-III (Fig. 10), presented the highest stress values at the medial pterygoid plate, mini-screw area, and lateral pterygoid plate (350.8 MPa, 306.7 MPa and 67.99 MPa, respectively). Model-I (Fig. 8), displayed the highest stress values measured at the medial pterygoid plate (67.99 MPa) and the lateral pterygoid plate (9.68 MPa), respectively.



(a) (b)

Fig. 4. Displacement of the landmarks due to SARPE after 5 mm activation of the expander apparatus for the Model-I: frontal view simulation (A) and occlusal view simulation (B).

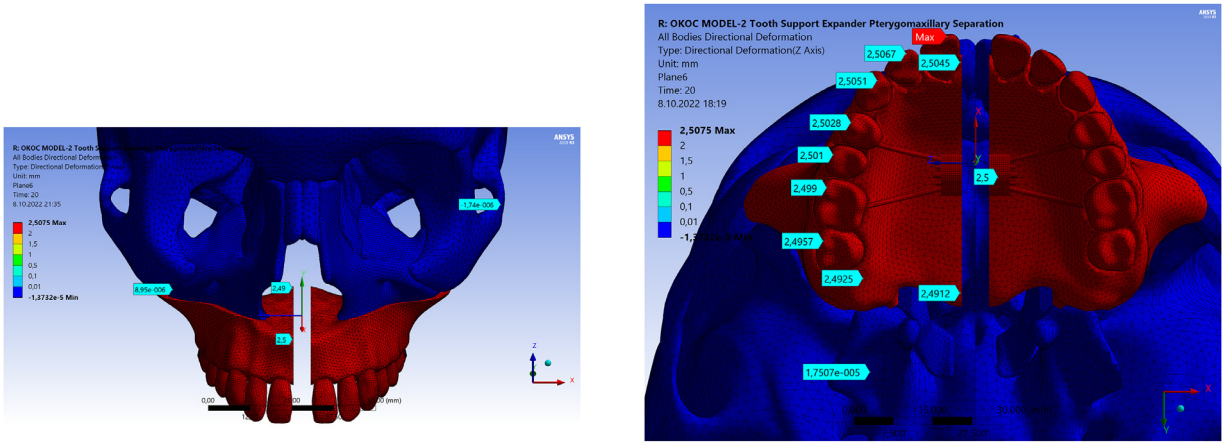


Fig. 5. Displacement of the landmarks due to SARPE after 5 mm activation of the expander apparatus for the Model-II: frontal view simulation (A) and occlusal view simulation (B).

The mean elemental stress (von Mises stress) values, ranked from highest to lowest, were observed at medial pterygoid plate, miniscrew region, lateral pterygoid plate, first molar tooth and frontozygomatic suture for Model-III (Table 4). Model-II (Fig. 9) and Model-IV (Fig. 11), due to the surgical technique, presented tension values in the craniofacial and maxillofacial structures decreasing dramatically (nearly zero). Stress value at the first molar teeth was found to be higher in Model-III (Fig. 10) than in Model-I (Fig. 8) being measured as 18.31 MPa and 4.08 MPa, respectively.

Structural error and singularity

When the maximum stress zones (red-color in figures) are examined, it can be seen that stress accumulates at nodes and on a few elements of that volume (singularity error). Maximum mean elemental stress (MMES) values were high. Model-III presented the highest MMES value (896 MPa) at the area of the most distal miniscrew (Fig. 10C), and the Model-I showed the highest MMES value, in a single element (217 MPa) at the pterygomaxillary junction (Fig. 8D).

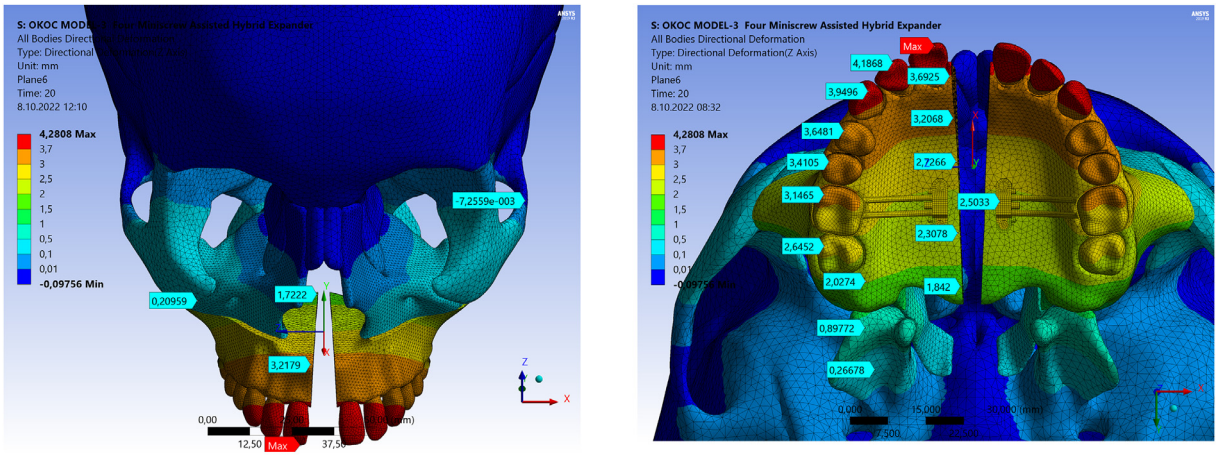


Fig. 6. Displacement of the landmarks due to SARPE after 5 mm activation of the expander apparatus for the Model-III: frontal view simulation (A) and occlusal view simulation (B).

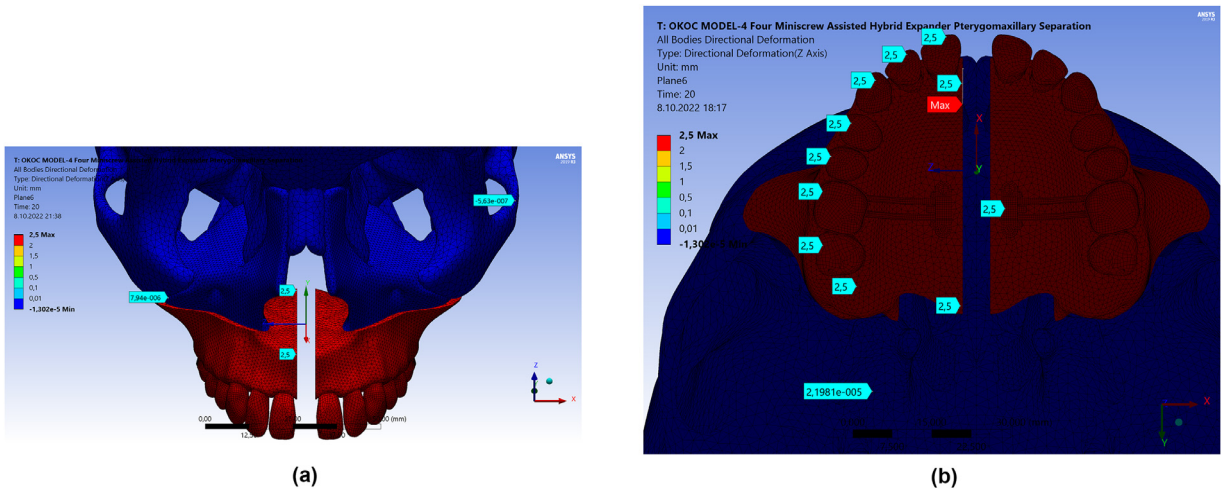


Fig. 7. Displacement of the landmarks due to SARPE after 5 mm activation of the expander apparatus for the Model-IV: frontal view simulation (A) and occlusal view simulation (B).

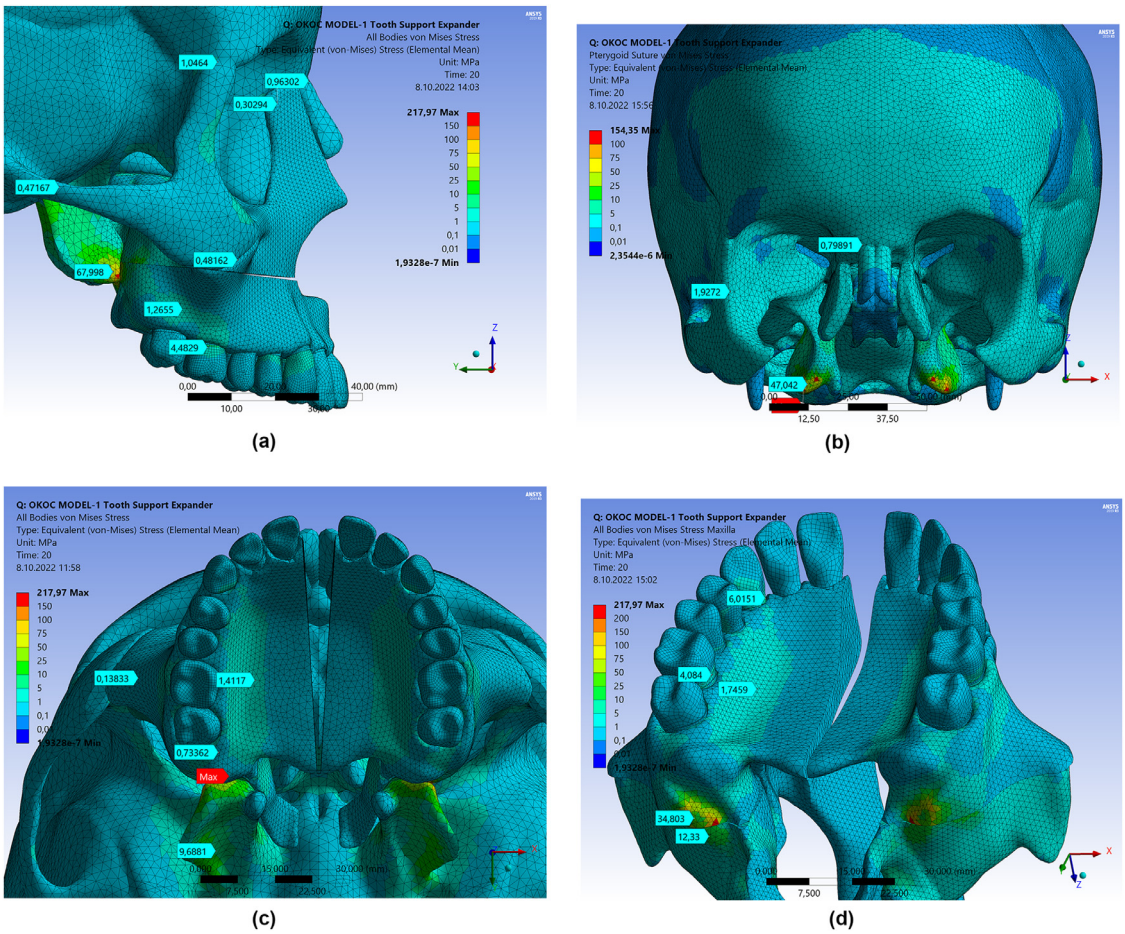


Fig. 8. Model-I: stress distribution in the craniofacial structures and maxillofacial sutures after 5 mm activation of the palatal expander. Lateral view (A), frontal view (B), occlusal view (C), and occluso-dorsal/pterygomaxillary suture view (D).

Table 4. The mean elemental stress (von Mises stress and first principal stress) distribution of the evaluated structures after 5 mm of the maxillary expander activation.

Structure	*Model-I* *Von Mises Stress (MPa)*	*First Principal Stress (MPa)*	*Model-II* *Von Mises Stress (MPa)*	*First Principal Stress (MPa)*	*Model-III* *Von Mises Stress (MPa)*	*First Principal Stress (MPa)*	*Model-IV* *Von Mises Stress (MPa)*	*First Principal Stress (MPa)*
Frontomaxillary suture	0.302	0.191	0.000	0.000	11.040	2.420	0.000	0.000
Zygomaticomaxillary suture	0.481	0.011	0.002	0.000	14.570	2.300	0.000	0.000
Frontozygomatic suture	1.046	-0.073	0.001	-0.000	49.930	-3.640	0.001	-0.000
Zygomatic arch	0.471	0.013	0.003	0.002	35.200	13.900	0.001	0.002
Nasal frontal suture	0.963	1.300	0.001	-0.000	18.490	21.600	0.000	0.000
Medial pterygoid plate	67.990	10.400	0.001	0.000	350.800	108.000	0.001	0.000
Lateral pterygoid plate	9.688	1.340	0.005	0.001	145.900	46.800	0.013	0.005
Maxillary tuberosity	0.733	0.602	0.000	0.000	35.520	19.700	0.001	0.001
Posterior nasal spine	0.011	0.011	0.000	0.000	5.130	5.000	0.000	0.000
Anterior nasal spine	0.006	0.005	0.000	0.000	0.248	0.014	0.000	0.000
Miniscrew region	-	-	-	-	306.700	251.000	0.053	0.009
First molar	4.084	-0.363	0.014	0.001	18.310	11.300	0.001	0.000

Obs.: Positive (+) values indicate compression stress and negative (−) values indicate tensile stress; MPa=megapascal.

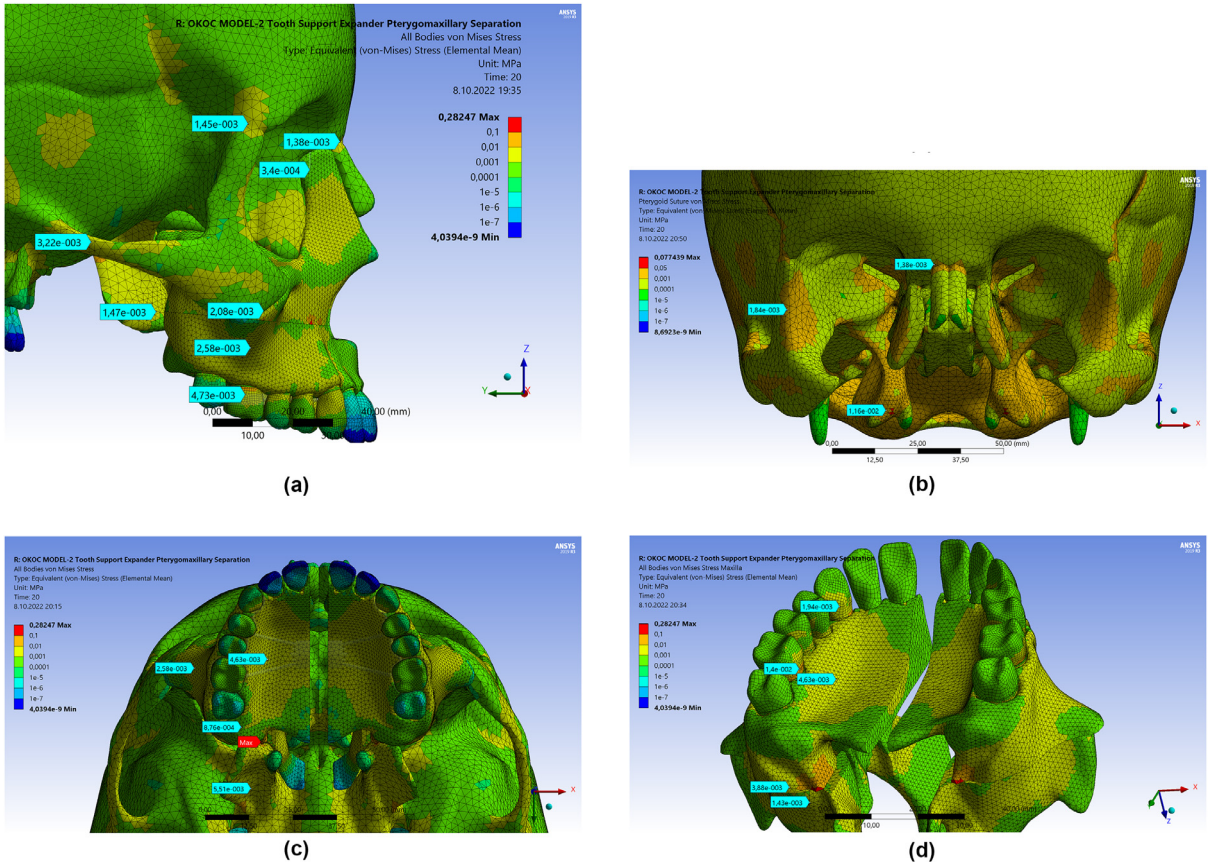


Fig. 9. Model-II: stress distribution in the craniofacial structures and maxillofacial sutures after 5 mm activation of the palatal expander. Lateral view (A), frontal view (B), occlusal view (C), and occluso-dorsal/pterygomaxillary suture view (D).

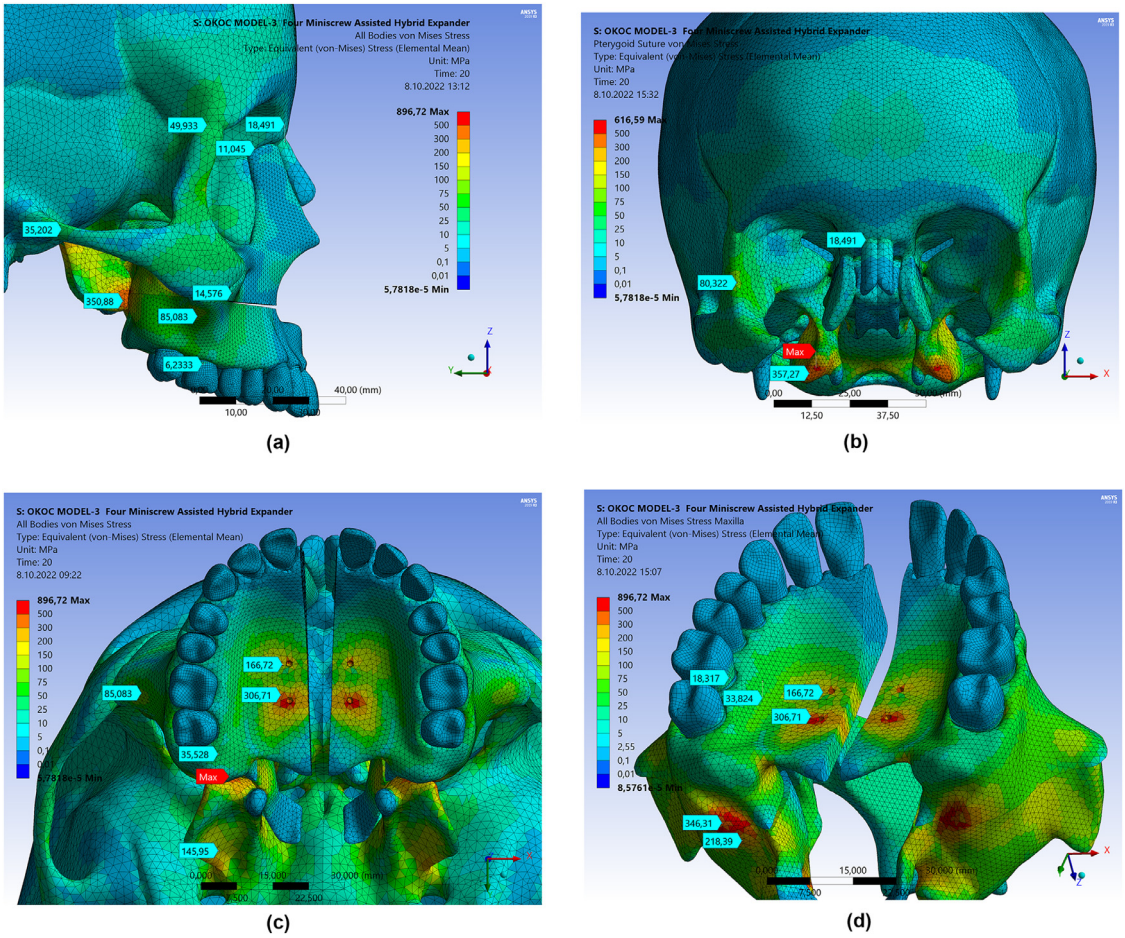


Fig. 10. Model-III: stress distribution in the craniofacial structures and maxillofacial sutures after 5 mm activation of the palatal expander. Lateral view (A), frontal view (B), occlusal view (C), and occluso-dorsal/pterygomaxillary suture view (D).

Discussion

Finite element simulation

Finite element analysis is a standard engineering method used to evaluate the amount of stress and displacement of complex geometric structures. This study includes a mathematical model based on human skull and it represents a clinical simulation of an adult patient to rationalize different treatment modalities, including evaluation of surgical procedures such as SARPE. By defining accurately modeled anatomical structure, boundary conditions and material properties, clinical situation can be simulated and comparable with different expansion appliance designs and/or surgical osteotomy methods.[51,52–54]

Numerous assumptions and simplifications in FEM/FEA can reduce the model's accuracy. The anchor miniscrew of the maxillary expander device and the craniofacial structure were not fully modeled in some studies.[50–52,55–60] In addition, some studies did not mention the boundary condition between bone, PDL, tooth, and expansion appliance. It is important to give these boundary conditions in order to compare the results in future FEM studies.[50–52,55–60] For reliable and reproducible results in FEM/FEA studies, it is very important to specify the boundary conditions (displacement amount, contact type, applied forces), material properties, mesh element-node numbers and mesh convergence, which expresses a sufficient number of elements that should be present in the model.[34,35,54,61–63]

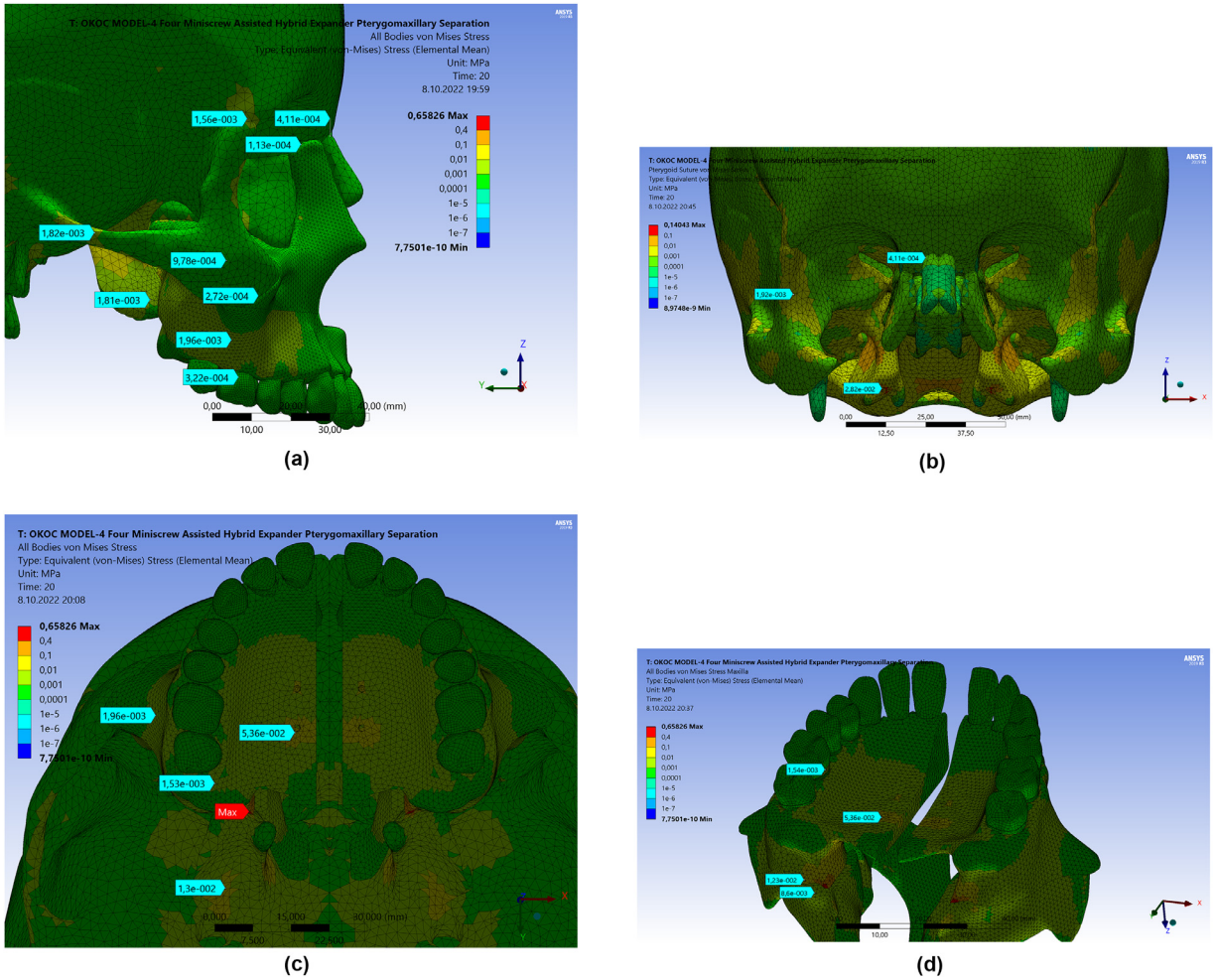


Fig. 11. Model-IV: stress distribution in the craniofacial structures and maxillofacial sutures after 5 mm activation of the palatal expander. Lateral view (A), frontal view (B), occlusal view (C), and occluso-dorsal/pterygomaxillary suture view (D).

For a better understanding of the study's quality, the skewness mesh metrics spectrum (Fig. 12) is significant. The accuracy of the analysis results is affected by low orthogonal quality and high skewness values and are not recommended.[62,63] The accuracy decreases as the average skewness value decreases from excellent to good. The average mesh convergence value and skewness element quality of our model were excellent in the entire bone structure constituting the geometry, and were very good for PDL, tooth, and expansion appliance. Quadratic hexahedral element mesh structure is preferred since the force is transmitted directly to the maxilla through the teeth and PDL. The FEA mesh has a direct effect on the accuracy of the solution in the model. In some FEM/FEA studies in the literature, incomplete and no-smooth geometric models were used, and mesh structure (element size, number of nodes), mesh convergence, boundary

Excellent	Very good	Good	Acceptable	Bad	Unacceptable
0-0.25	0.25-0.50	0.50-0.80	0.80-0.94	0.95-0.97	0.98-1.00

Fig. 12. Skewness mesh metrics spectrum.

conditions, and expansion appliance type were not specified.[15,50,52,55,56,59,64] Therefore, comparison is problematic, and careful consideration of the findings from earlier literature is essential.

In order to obtain more reliable and accurate results in FEM/FEA studies, a nonlinear analysis method and a protocol similar to the clinical activation of the screw are recommended.[32,51,64] Unlike the clinical scenario in previous SARPE/FEM studies, the amount of tension and displacement in the craniofacial and maxillofacial sutures was evaluated with the initial movement of the expansion screw (0.25−1 mm) [53,61,64] and the screw force (60 N).[65] In our study, a symmetrical model with a total of 5.00 mm (20 activations of the expander screw) widening was performed to better reflect the clinical situation, and nonlinear analysis (three theories) method was used. The effect of the expansion appliance on the craniofacial and maxillofacial structure was examined depending on time (20 seconds total). Transient structural analysis (dynamic analysis) can be used to find the dynamic response (displacement, strain, stress, and forces) of a structure under the influence of any general time-varying, transient load.[63] There is no FEA study that moves the expansion appliance screw directly/total 5 mm in simulation of hyrax- or hybrid-assisted expansion with or without pterygomaxillary suture osteotomy in SARPE.

In models without pterygomaxillary suture separation, the highest stress values were measured in the medial and lateral pterygoid plates, except for the miniscrew area. In the models with pterygomaxillary suture separation, the stress value approached zero because all the resistance regions were removed. Interesting, the stress value measured in the first molar tooth in Model-III (a tooth-bone-borne palatal expander type) is higher than in Model-I (Hyrax). In Model-I, the expansion device transmits/distributes the screw movement/force over teeth and PDL. In Model-III, force acts on a single tooth and PDL. At the same time, the bone and appliance anchored screw slightly flex and/or move. Due to the slight movement, the force is transferred to the molar tooth through the double appliance arms and may result in a higher measurement of the stress. In tooth-supported expansion appliances, getting support from as many teeth as possible causes less tipping and rotation of the teeth.

The stress and displacement values measured from the craniofacial and maxillofacial sutures were found to be relatively similar in studies using FEA to simulate hybrid or hyrax-assisted expansion in SARPE, with and without PTMS. Results can differ depending mainly on the accuracy of the model used, surgical osteotomy method, type of expansion appliance, anchor screw position, material properties, mesh structure, and boundary conditions.[30,40,65]

Clinical findings

Regardless of the maxillary expander device type, both SARPE techniques (with and without PMS osteotomy) effectively produces maxillary expansion. SARPE with PMS osteotomy presented parallel maxillary expansion, while the absence of the PMS osteotomy produced a V-shaped expansion. It has been suggested that the resistance of transverse maxillary expansion is the zygomaticomaxillary buttress and the pterygomaxillary junction.[28] Eliminating the resistance to lateral movement by osteotomy should allow for larger posterior maxillary basal bone movement. A uniform maxillary expansion in the anteroposterior plane has been shown when PMS osteotomy is performed.[66] Dental and skeletal V-shaped expansion has been reported regardless of the osteotomy technique.[57,58] Trying to reconciliate the differences, a meta-analysis showed that anterior and posterior expansions did not differ meaningfully when SARPE was associated or not to PMS osteotomy.[67] Comparisons are problematic because the amount and shape of the maxillary expansion may vary depending on some biomechanical factors such as surgical technique, use of different expansion apparatus location, patient's age maturation, and bone/midpalatal suture density.

Pterygomaxillary osteotomy reduces tension values and stresses at craniofacial structures dramatically. Regardless of the maxillary expander type, the areas and levels of stress were reduced to the point where they were negligible when SARPE was performed associated with PMS osteotomy. Some authors mentioned that the osteotomies are more important in reducing stress in certain areas than the type of the device.[52,56] In addition, the literature has shown that additional pterygomaxillary junction release procedure reduces stress near cranial base and/or anchor teeth.[51,53,56] The relatively low stress values in the maxillofacial sutures reduces the

chance of small cracks or fractures. Results on the strain and displacement of craniofacial structures were relatively similar to FEA studies on the SARME.[61,62,64] Additionally, the suggestion of the pterygomaxillary disjunction in our study confirmed the results in previous studies.[34,35,66] Some studies have shown that the areas with the highest resistance to expansion were the midpalatal suture, zygomaticomaxillary, zygomatic arch, frontomaxillary suture, and PMS in the craniofacial structure.[39,68,69] In our study, the highest areas of resistance were the PMS, miniscrew area, and zygomatic arch region. These results were consistent with those of the previous studies.[53,56,61,64]

Clinical implications

It seems that the surgical technique could play important role on pterygoid plates displacement,[51–53] but surgeons are concerned about of the advantages of the pterygomaxillary disjunction due to increasing of fractures in adjacent bones or injuring the vasculature in the posterior of the maxilla.[22]

If transverse maxillary expansion is needed more anteriorly than posteriorly, only lateral and median osteotomy should be performed without PMS osteotomy while additional PMS separation should be sufficient for a parallel transverse maxillary expansion. In addition, there is a possibility that relapse might be reduced by a reduction in the stress values, thus improving the stability of the transverse maxillary expansion.

With pterygomaxillary osteotomy, the stress values in the craniofacial structures have significantly reduced, and a parallel enlargement pattern was seen in the anteroposterior plane of the maxilla. It can be expected that the amount of relapse will decrease due to the decrease in the stress in the craniofacial and maxillofacial structures. The expander type can be recommended according to the required maxillary expansion pattern and displacement. These SARPE-FEM/FEA simulation results may be helpful and instructive for the clinical application, but *in-vivo* studies are required to confirm these results.

Limitations and Verification

In this FEA simulation, bone remodeling, relapse after expansion, muscles and chewing forces, effects of soft tissues, were not included in the analysis. If these factors could be added to the boundary conditions, the simulation's accuracy should improve. As a result, the displacement and stress values may be greater than the clinical values, and our findings may differ from the clinical results. The highest stress values were observed in the pterygomaxillary suture and mini-screw insertion areas, and the maximum stress values that occurred were extremely high. These values (singularity), a function of the FEM/FEA procedure, were measured in a few (red colored) elements of the volume and knot components of the pterygomaxillary suture and mini-screw region. The maximum stress value due to the singularity error was not considered. Therefore, it did not affect the results measured in the analysis. In areas with sharp corners high stress values occur due to the mathematical calculation errors in FEA.[35,63,65,66] Singularity refers to the position where the stress value is unlimited in the finite element model. There is no stress singularity in a real structure. Situations in which a stress singularity occurs can be boundary conditions (application of a point load) or geometry of the model (simplification, surfaces with non-uniform sharp corners and edges).[63] In the bone model, there are non-uniform sharp-edged surfaces due to geometry.

Element mesh quality is essential to verify skewness values, and determines how close the elements that make up the model are to the ideal. In this study, the skewness element quality value of the bones forming the maxilla and skull was excellent (Table 2).

In the FEM method, it is known that the geometry is divided into small elements.

The accuracy of the solution largely depends on the element mesh size and quality of the elements into which the model is divided. As we progressively refine the mesh that composes the elements in the model (dividing it into smaller elements), the solution improves and given enough iterations it converges towards a specific result. Even if the element size is reduced after a point, the solution result does not change. There are also cases where the solution does not converge with mesh refinement. Stress singularity is one of these situations.

Furthermore, due to the flexibility of the bone against loads and its self-healing feature, the maximum stress value does not actually

accumulate at a single point as in the analysis result.[35,63,65,66]

Conclusions

Based on the finite element method/finite element analysis, surgical assisted rapid palatal expansion, with or without pterygomaxillary osteotomy, effectively produced a maxillary expansion, regardless of the expander design. In addition, the following conclusions can be drawn:

- The pterygomaxillary suture (PMS) separation presented parallel maxillary expansion, while the absence of the PMS osteotomy produced a V-shaped expansion;
- SARPE associated with PMS osteotomy might reduce the stress values in the craniofacial and maxillofacial structure to nearly zero.

Patient consent

Consent to publish the case report was obtained.

Funding

No funding or grant support.

Author contributions

All authors attest that they meet the current ICMJE criteria for Authorship.

Declaration of competing interest

The authors declare that they have no known competing financial interests or personal relationships that could have appeared to influence the work reported in this paper.

Supplementary materials

Supplementary material associated with this article can be found in the online version at doi:10.1053/j.sodo.2022.10.017.

References

1. Langlois JH, Kalakanis L, Rubenstein AJ, Larson A, Hallam A, Smoot M. Maxims or myths of beauty? A meta-analytic and theoretical review. *Psychol Bull*. 2000;126:390–423.
2. Hosoda M, Stone-Romero EF, Coats G. The effects of physical attractiveness on job-related outcomes: a meta-analysis of experimental studies. *Personnel Psychol*. 2003;56:431–462.
3. Roden-Johnson D, Gallerano R, English J. The effects of buccal corridor spaces and arch form on smile esthetics. *Am J Orthod Dentofacial Orthop*. 2005;127:343–350.
4. Parekh SM, Fields HW, Beck M, Rosenstiel S. Attractiveness of variations in the smile arc and buccal corridor space as judged by orthodontists and laymen. *Angle Orthod*. 2006;76:557–563.
5. Oshagh M, Zarif NH, Bahramnia F. Evaluation of the effect of buccal corridor size on smile attractiveness. *Eur J Esthet Dent*. 2010;5:370–380.
6. Moore T, Southard KA, Casko JS, Qian F, Southard TE. Buccal corridors and smile esthetics. *Am J Orthod Dentofacial Orthop*. 2005;127:208–213.
7. Ritter DE, Gandini LG, Pinto A dos S, Locks A. Esthetic influence of negative space in the buccal corridor during smiling. *Angle Orthod*. 2006;76:198–203.
8. Martin AJ, Buschang PH, Boley JC, Taylor RW, McKinney TW. The impact of buccal corridors on smile attractiveness. *Eur J Esthet Dent*. 2007;29:530–537.
9. McNamara L, Mc Jr NJA, Ackerman MB, Baccetti T. Hard and soft-tissue contributions to the esthetics of the posed smile in growing patients seeking orthodontic treatment. *Am J Orthod Dentofacial Orthop*. 2008;133:491–499.
10. Carvalho A, Goldenberg FC, Angelieri F, et al. Assessment of changes in smile after rapid maxillary expansion. *Dental Press J Orthod*. 2012;17:94–101.
11. Shook C, Kim SM, Burnheimer J. Maxillary arch width and buccal corridor changes with Damon and conventional brackets: a retrospective analysis. *Angle Orthod*. 2016;86:655–660.
12. Proffit WR. Prevalence of malocclusion and orthodontic treatment need in the United States: estiamates from the NHANES III survey. *Int J Adult Orthod Orthognath Surg*. 1998;13:97–106.
13. Betts NJ, Vanarsdall RL, Barber HD, Higgins-Barber K, Fonseca RJ. Diagnosis and treatment of transverse maxillary deficiency. *Int J Adult Orthodon Orthognath Surg*. 1995;10:75–96.
14. Carvalho PHA, Moura LB, Trento GS, Holzinger D, Gabrielli MAC, Gabrielli MFR, Pereira Filho VA. Surgically assisted rapid maxillary expansion: a systematic review of complications. *Int J Oral Maxillofac Surg*. 2020;49:325–332.
15. Verstraaten J, Kuijpers-Jagtman AM, Mommaerts MY, Bergé SJ, Nada RM, Schols JG, Eurocran Distraction Osteogenesis Group. A systematic review of the effects of bone-borne surgical assisted rapid maxillary expansion. *J Craniomaxillofac Surg*. 2010;38:166–174.
16. Yoon S, Lee DY, Jung SK. Influence of changing various parameters in miniscrew-assisted rapid palatal expansion: a three-dimensional finite element analysis. *Korean J Orthod*. 2019;49:150–160.
17. Lin L, Ahn HW, Kim SJ, Moon SC, Kim SH, Nelson G. Tooth-borne vs bone-borne rapid maxillary expanders in late adolescence. *Angle Orthod*. 2015;85:253–262.
18. Seong EH, Choi SH, Kim HJ, HS Yu, Park YC, Lee KJ. Evaluation of the effects of miniscrew incorporation in

palatal expanders for young adults using finite element analysis. *Korean J Orthod*. 2018;48:81–89.
19. Lines PA. Adult rapid maxillary expansion with corticotomy. *Am J Orthod*. 1975;67(1):44–56.
20. Proffit WR, Turvey TA, Phillips C. Orthognathic surgery: a hierarchy of stability. *Int J Adult Orthodon Orthognath Surg*. 1996;11:191–204.
21. Pogrel MA, Kaban LB, Vargervik K, Baumrind S. Surgically assisted rapid maxillary expansion in adults. *Int J Adult Orthodon Orthognath Surg*. 1992;7:37–41.
22. Koudstaal MJ, Poort LJ, van der Wal KG, Wolvius EB, Prahl-Andersen B, Schulten AJ. Surgically assisted rapid maxillary expansion (SARME): a review of the literature. *Int J Oral Maxillofac Surg*. 2005;34:709–714.
23. Holberg C, Rudzki-Janson I. Stresses at the cranial base induced by rapid maxillary expansion. *Angle Orthod*. 2006;76:543–550.
24. Kokich VG. Age changes in the human frontozygomatic suture from 20 to 95 years. *Am J Orthod*. 1976;69:411–430.
25. Turvey TA. Maxillary expansion: a surgical technique based on surgical-orthodontic treatment objectives and anatomical considerations. *J Maxillofac Surg*. 1985;13:51–58.
26. Handelman CS. Nonsurgical rapid maxillary alveolar expansion in adults: a clinical evaluation. *Angle Orthod*. 1997;67:291–305. discussion 306–8.
27. Byloff FK, Mossaz CF. Skeletal and dental changes following surgically assisted rapid palatal expansion. *Eur J Orthod*. 2004;26:403–409.
28. Suri L, Taneja P. Surgically assisted rapid palatal expansion: a literature review. *Am J Orthod Dentofacial Orthop*. 2008;133:290–302.
29. Lehman Jr. JA, Haas AJ, Haas DG. Surgical orthodontic correction of transverse maxillary deficiency: a simplified approach. *Plast Reconstr Surg*. 1984;73:62-8.
30. Bays RA, Greco JM. Surgically assisted rapid palatal expansion: an outpatient technique with long-term stability. *J Oral Maxillofac Surg*. 1992;50:110-3.
31. Betts NJ, Ziccardi VB. Surgically assisted maxillary expansion. In: Fonseca RJ, ed. *Oral and maxillofacial surgery*. Philadelphia: W. B. Saunders; 2000:211–231.
32. Seeberger R, Kater W, Davids R, Thiele OC. Long term effects of surgically assisted rapid maxillary expansion without performing osteotomy of the pterygoid plates. *J Craniomaxillofac Surg*. 2010;38:175-8.
33. Sygouros A, Motro M, Ugurlu F, Acar A. Surgically assisted rapid maxillary expansion: cone-beam computed tomography evaluation of different surgical techniques and their effects on the maxillary dentoskeletal complex. *Am J Orthod Dentofacial Orthop*. 2014;146:748-57.
34. Möhlhenrich SC, Ernst K, Peters F, et al. Immediate dental and skeletal influence of distractor position on surgically assisted rapid palatal expansion with or without pterygomaxillary disjunction. *Int J Oral Maxillofac Surg*. 2021;50:649–656.
35. Sankar SG, Prashanth B, Rajasekhar G, Prasad M, Reddy GV, Priyanka JS. A comparison of different osteotomy techniques with and without pterygomaxillary disjunction in surgically assisted maxillary expansion utilizing modified hybrid rapid maxillary expansion device with posterior implants: a finite element study. *Natl J Maxillofac Surg*. 2021;12:171–180.
36. Glassman AS, Nahigian SJ, Medway JM, Aronowitz HI. Conservative surgical orthodontic adult rapid palatal expansion: sixteen cases. *Am J Orthod*. 1984;86:207–213.
37. Basdra EK, Zöller JE, Komposch G. Surgically assisted rapid palatal expansion. *J Clin Orthod*. 1995;29:762–766.
38. Anttila A, Finne K, Keski-Nisula K, Somppi M, Panula K, Peltomäki T. Feasibility and long-term stability of surgically assisted rapid maxillary expansion with lateral osteotomy. *Eur J Orthod*. 2004;26:391–395.
39. Bell WH, Jacobs JD. Surgical-orthodontic correction of horizontal maxillary deficiency. *J Oral Surg*. 1979;37:897–902.
40. Alpern MC, Yurosko JJ. Rapid palatal expansion in adults with and without surgery. *Angle Orthod*. 1987;57:245–263.
41. Mehra P, Cottrell DA, Caiazzo A, Lincoln R. Life-threatening, delayed epistaxis after surgically assisted rapid palatal expansion: a case report. *J Oral Maxillofac Surg*. 1999;57:201–204.
42. Nagaoka T, Watanabe S. Postured voxel-based human models for electromagnetic dosimetry. *Phys Med Biol*. 2008;53(24):7047–7061. https://doi.org/10.1088/0031-9155/53/24/003.
43. National bioscience database center, "BodyParts3D, The Database Center for Life Science Licensed under CC Attribution-Share alike 2.1 Japan", National bioscience database center. https://dbarchive.biosciencedbc.jp/en/bodyparts3d/desc.html (Accessed: March 3, 2018).
44. Nagaoka T, Watanabe S, Sakurai K, et al. Development of realistic high-resolution whole-body voxel models of Japanese adult males and females of average height and weight, and application of models to radio-frequency electromagnetic-field dosimetry. *Phys Med Biol*. 2004;49:1–15.
45. Mitsuhashi N, Fujieda K, Tamura T, Kawamoto S, Takagi T, Okubo K. BodyParts3D: 3D structure database for anatomical concepts. *Nucleic Acids Res*. 2009;37(Database issue):D782–D785.
46. Kronfeld R. Histologic study of the influence of function on the human periodontal membrane. *J Am Dent Assoc*. 1931;18:1242–1274.
47. Hong C, Lee H, Webster R, Kwak J, Wu BM, Moon W. Stability comparison between commercially available miniimplants and a novel design: part 1. *Angle Orthod*. 2011;81:692–699.
48. Peterson J, Wang Q, Dechow PC. Material properties of the dentate maxilla. Anat. Rec. Part A. *Discov. Mol. Cell. Evol. Biol. An Off. Publ. Am. Assoc. Anat*. 2006;88:962–972.
49. Ortún-Terrazas J, Cegoñino J, Santana-Penín U, Santana-Mora U, Pérez Del Palomar A. Approach towards the porous fibrous structure of the periodontal ligament using micro-computerized tomography and finite element analysis. *J Mech Behav Biomed Mater*. 2018;79:135–149.
50. Gautam P, Valiathan A, Adhikari R. Stress and displacement patterns in the craniofacial skeleton with rapid maxillary expansion: a finite element method study. *Am J Orthod Dentofacial Orthop*. 2007;132. 5.e1-5.e11.
51. Han UA, Kim Y, Park JU. Three-dimensional finite element analysis of stress distribution and displacement of the maxilla following surgically assisted rapid maxillary expansion. *J Craniomaxillofac Surg*. 2009;37:145–154.

52. de Assis DS, Xavier TA, Noritomi PY, Gonçales AG, Ferreira Jr O, de Carvalho PC. Gonçales ES. Finite element analysis of stress distribution in anchor teeth in surgically assisted rapid palatal expansion. *Int J Oral Maxillofac Surg*. 2013;42:1093–1099.
53. Lee SC, Park JH, Bayome M, Kim KB, Araujo EA, Kook YA. Effect of bone-borne rapid maxillary expanders with and without surgical assistance on the craniofacial structures using finite element analysis. *Am J Orthod Dentofacial Orthop*. 2014;145:638–648.
54. Romanyk DL, Vafaeian B, Addison O, Adeeb S. The use of finite element analysis in dentistry and orthodontics: critical points for model development and interpreting results. *Semin Orthod*. 2020;26:162–173.
55. Chaconas SJ, Caputo AA. Observation of orthopedic force distribution produced by maxillary orthodontic appliances. *Am J Orthod*. 1982;82:492–501.
56. Holberg C, Steinhäuser S, Rudzki I. Surgically assisted rapid maxillary expansion: midfacial and cranial stress distribution. *Am J Orthod Dentofacial Orthop*. 2007;132:776–782.
57. Chamberland S, Proffit WR. Closer look at the stability of surgically assisted rapid palatal expansion. *J Oral Maxillofac Surg*. 2008;66:1895–1900.
58. Kilic E, Kilic B, Kurt G, Sakin C, Alkan A. Effects of surgically assisted rapid palatal expansion with and without pterygomaxillary disjunction on dental and skeletal structures: a retrospective review. *Oral Surg Oral Med Oral Pathol Oral Radiol*. 2013;115:167–174.
59. MacGinnis M, Chu H, Youssef G, Wu KW, Machado AW, Moon W. The effects of micro-implant assisted rapid palatal expansion (MARPE) on the nasomaxillary complex – a finite element method (FEM) analysis. *Prog. Orthod.*. 2014;15:1–15.
60. Haas Junior OL, Matje PRB, Rosa BM, et al. Minimally invasive surgical and miniscrew-assisted rapid palatal expansion (MISMARPE) in adult patients. *J Craniomaxillofac Surg*. 2022;50:211–217.
61. Möhlhenrich SC, Modabber A, Kniha K, et al. Simulation of three surgical techniques combined with two different bone-borne forces for surgically assisted rapid palatal expansion of the maxillofacial complex: a finite element analysis. *Int J Oral Maxillofac Surg*. 2017;46:1306–1314.
62. Lee RJ, Moon W, Hong C. Effects of monocortical and bicortical mini-implant anchorage on bone-borne palatal expansion using finite element analysis. *Am J Orthod Dentofac Orthop*. 2017;151:887–897.
63. Bi Z. Finite element analysis applications, a systematic and practical approach. Bi Z., ed.. *Chapter 12-Validation and verification*. Academic Press; 2018:455–494. pages.
64. Lee HK, Bayome M, Ahn CS, Kim SH, Kim KB, Mo SS, Kook YA. Stress distribution and displacement by different bone-borne palatal expanders with micro-implants: a three-dimensional finite-element analysis. *Eur J Orthod*. 2014;36:531–540.
65. de Assis DS, Xavier TA, Noritomi PY. Gonçales ES. Finite element analysis of bone stress after SARPE. *J Oral Maxillofac Surg*. 2014;72. 167.e1-167.e1677.
66. Zandi M, Miresmaeili A, Heidari A, Lamei A. The necessity of pterygomaxillary disjunction in surgically assisted rapid maxillary expansion: a short-term, double-blind, historical controlled clinical trial. *J Craniomaxillofac Surg*. 2016;44:1181–1186.
67. Hamedi Sangsari A, Sadr-Eshkevari P, Al-Dam A, Friedrich RE, Freymiller E, Rashad A. Surgically assisted rapid palatomaxillary expansion with or without pterygomaxillary disjunction: a systematic review and meta-analysis. *J Oral Maxillofac Surg*. 2016;74:338–348.
68. Lines PA. Adult rapid maxillary expansion with corticotomy. *Am J Orthod*. 1975;67:44–56.
69. Timms DJ, Vero D. The relationship of rapid maxillary expansion to surgery with special reference to midpalatal synostosis. *Br J Oral Surg*. 1981;19:180–196.